ACS OMEGA

http://pubs.acs.org/journal/acsodf

Article

Design and Preparation of Ethylene Fluorescence Probes Based on Arylolefins and Grubbs Catalysts

Yanyan Yang, Hongxia Bian, Zhilong Jia, and Peng Tu*

Cite This: *ACS Omega* 2023, 8, 15350−15359

Read Online

ACCESS | Metrics & More | Article Recommendations | Supporting Information

ABSTRACT: To detect the plant hormone ethylene, three arylolefins were employed to react with ethylene based on olefin metathesis. In this study, three fluorescence probes were successfully prepared using a first-generation Grubbs catalyst (G-1) and arylolefin with terminal vinyl groups. The probes were characterized using various techniques, including UV−vis, fluorescence, FT-IR, ^{1}H NMR, ^{13}C NMR, and ^{31}P NMR spectroscopies and HRMS. The probes exhibited an emission maximum at 394 nm and showed excellent ethylene response. The detection limits for the probes were calculated to be 0.128, 0.074, and 0.188 μL/mL (3σ), respectively, based on fluorescence stimulation by ethylene gas. Additionally, the YGTZ-2 probe was used to detect ethylene gas during the storage process of tomatoes. This work expands the application of arylolefin in ethylene detection and provides a foundation for the development of economic, rapid, and convenient photosensitive sensors for ethylene in the future.

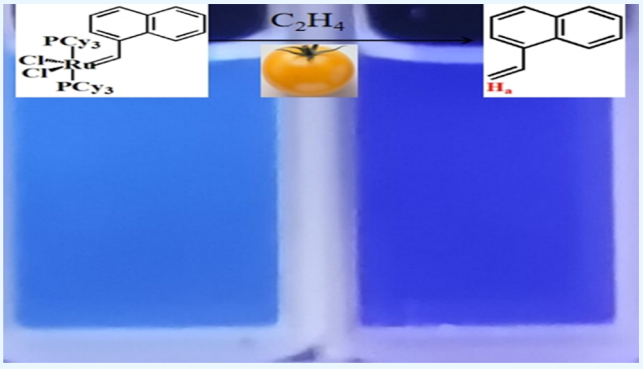

1. INTRODUCTION

Ethylene, an inscrutable gaseous hormone prevalent in plants, is known to bring about a triple response, as well as partial growth. It is no wonder then that this plant hormone is often dubbed the mature hormone.[1,2] Ethylene, being the crucial agent that governs the fruit's size, kick-starts and advances fruit maturation as it blossoms into its desired size.[3] This incredible feat is attributed primarily to ethylene's ability to augment the permeability of plasma membrane, bolster the activity of hydrolase, hasten the respiration oxidation decomposition, and facilitate the rapid transformation of organic matter in pulp to reach the perfect edibility.[4−6] Therefore, keeping a watchful eye on the release of ethylene during the fruit ripening process is paramount in ensuring quality control. Failure to do so could result in massive economic losses for fruit growers and a tremendous waste of resources.[7,8] To avoid such calamitous consequences, researchers have delved into establishing cutting-edge methodologies for detecting ethylene. The most commonly employed approaches for monitoring ethylene levels include gas chromatography, photoacoustic spectroscopy, and electrochemical techniques.[9,10] Nonetheless, the methods mentioned earlier entail intricate sample preprocessing and a slew of other perplexing steps, rendering their use process cumbersome and impractical for promotion in agriculture.[11] To circumvent this predicament, the principle of photoluminescence comes into play. By harnessing the photoluminescence characteristics of the material, the preprocessing step of the detected sample can be simplified, and the sample can be directly detected.[12,13] In recent years, the fluorescence probe method based on the principle of photoluminescence has garnered the interest of researchers.[14,15] These fluorescent probes boast of being economical, convenient, speedy, and adept at preserving the freshness and texture of fruits.[5] Fluorescent probes are substances that convert chemical information about intermolecular interactions into an effect on the fluorescent signal, thus enabling the recognition of specific molecules or ions. These probes can take on different forms, such as molecules, nanoparticles, aggregates, coordination polymers, and so on.[16] The recognition mechanisms of these fluorescent probes involve fluorescence enhancing or quenching, fluorescence characteristic peak position shift, fluorescence lifetime change, fluorescence polarization change, and more. Fluorescent probes operate through different mechanisms than the analyte, and their mode of action is mainly classified into internal conversion, intersystem crossing, and intermolecular interaction deactivation processes (involving electron transfer and energy transfer). The materials used to make fluorescent probes are primarily categorized into organic, inorganic, and organic−inorganic hybrid materials. Inorganic materials, for

Received: January 29, 2023
Accepted: April 7, 2023
Published: April 20, 2023

https://doi.org/10.1021/acsomega.3c00586
ACS Omega 2023, 8, 15350−15359

instance, are typically quantum dots, including carbon quantum dots, noble metal quantum dots, and semiconductor quantum dots.[17] Nagamalai Vasimalai proposed a method of protecting fluorescent gold nanodots with thiotetrazine to detect sulfides with a detection limit of 2 nM (S/N = 3).[18] Carbon quantum dots can be utilized in warm WLEDs and fluorescent ink applications, as well as security information encryption and anticounterfeiting applications.[19−21] Gold nanodots synthesized through a one-pot method can detect cyanide with a detection limit of 150 nM.[22] Currently, coordination compounds are the organic−inorganic hybrid materials most commonly employed in fluorescent sensing probes. The composition of coordination compounds is highly versatile, and the fluorescence spectrum can be adjusted by selecting appropriate organic ligands and metal ions. For instance, researchers utilized silver or copper to coordinate with conjugated organic compounds to construct fluorescent metallic complexes, thus developing fluorescent probes for observing ethylene.[23,24] Burstyn et al. selected $AgBF_4$, $AgSbF_6$, or $AgB(C_6F_5)_4$, dipped them in poly(vinyl ketone) or 1,4-bis(methyl styrene)benzene films, and demonstrated that ethylene gas could form coordination bonds with silver ions to generate fluorescence and produce a sensing response.[25] Indeed, the complex preparation processes and high cost of some fluorescent probes limit their industrial application. To overcome these challenges, researchers have been exploring simpler and more cost-effective approaches for developing fluorescent probes for ethylene detection. For example, Yutaka et al. established that the reversible interconversion between the metal−arene and metal−ethylene interactions allowed us to monitor ethylene.[26] Additionally, some researchers have explored the use of natural products, such as plant pigments, as fluorescent probes for ethylene detection. For instance, coumarins are a class of natural products with benzo α-pyranone nuclei, isolated in coumarbeans.[27] Ye et al. proposed coumarin, as the core of the fluorescent probe, coupled with ethylene/alcohol to structure a new C−H bond and organized correctly energetic sensing fluorescent probe to reveal ethylene launch from residing cells and plants. As a result, this probe's detection restriction reached 52 ppb.[28] The advantage of using natural products is that they are readily available, inexpensive, and environmentally friendly.

Using more cost-effective and higher yield fluorophores in the olefin metathesis of ethylene detection can definitely make fluorescent probes more useful in the agricultural and food industries. It is great to hear that Sun et al. were able to achieve a detection limit of 0.9 ppm for ethylene in the air using aromatic hydrocarbons 1-vinylpyrene as a fluorophore.[29] Our choice of 1-vinylnaphthalene and 1,1-diphenylethene as new fluorophores is promising, especially since 1-vinylnaphthalene has a smaller molecular weight than 1-vinylpyrene and can be used for various applications beyond just fluorescent probes.[30] We are interested to see the results of following experiments with these new fluorophores in ethylene detection. It is important to note that the development of simple and efficient fluorescent probes for ethylene detection can greatly benefit the transportation and storage of fruits, as well as provide more opportunities for fluorescence imaging of endogenous ethylene in plants. The characterization of the structure of the probes using FT-IR spectroscopy, HRMS, and ^{1}H NMR, ^{13}C NMR, and ^{31}P NMR spectroscopies, along with the testing of their ethylene response properties using UV−visible and fluorescence spectrophotometers, are crucial steps in the development of these probes. The monitoring of the ripening process of yellow tomatoes using these probes can provide valuable insights into the practical application of these probes in the agricultural industry. Overall, the development of cost-effective and sensitive fluorescent probes for ethylene detection can significantly improve the efficiency and quality of agricultural practices.

2. EXPERIMENTS

2.1. Materials and Methods. *2.1.1. Reagents and Instruments.* Chemical reagents are purchased from commercial sources and used directly. All glassware were cleaned with ultrapure water and dried before use. Fluorescence measurement was carried out by a fluorescence spectrophotometer (F-380 Tianjin Port East Technology Development Co. Ltd., China) with a plotter and a quartz colorimetric dish (1 cm × 1 cm). The UV absorption spectrum was recorded by a UV−visible spectrophotometer (TU-1901 Beijing Puxi General Instrument Co. Ltd., China). The process reaction was analyzed by thin layer chromatography (TLC) with an F_{254} silica gel 60 plates (Merck, Singapore).

2.1.2. Preparation of YGTZs. 2.1.2.1. Preparation of YGTZ−1. Methyltriphenylphosphine iodide (Ph_3PCH_3I), (8.08 g, 20 mmol) was dissolved in dry tetrahydrofuran (THF) (200 mL). Potassium *t*-butoxide (KO^tBu) (2.24 g, 20 mmol) was added into the solution at 0 °C and stirred for 30 min. Then, 1-pyrenecarboxaldehyde ($C_{17}H_{10}O$) (1.84 g, 8 mmol) was slowly added in two batches. The mixture was stirred for 6 h at room temperature and then 100 mL of deionized water was added to quench the reaction. The product of the reaction was extracted with ethyl acetate. Lastly, the organic layer was dried with sodium sulfate anhydrous, and white solid 1-vinylpyrene ($C_{18}H_{12}$) was obtain by column chromatography (developing agent: *n*-hexane/ethyl acetate = 10/1). ^{1}H NMR (600 MHz, Chloroform-*d*): δ 8.39 (s, 1H), 8.23−8.15 (m, 4H), 8.12 (d, J = 9.2 Hz, 1H), 8.05 (s, 2H), 8.00 (t, J = 7.6 Hz, 1H), 7.80 (dd, J = 17.3, 11.0 Hz, 1H), 6.00 (dd, J = 17.3, 1.1 Hz, 1H), 5.62 (dd, J = 11.0, 1.2 Hz, 1H). ^{13}C NMR (151 MHz, Chloroform-*d*): δ 134.13, 132.28, 131.38, 130.80, 128.01, 127.48, 127.35, 127.19, 125.86, 125.16, 124.93, 123.60, 122.94, 117.14.

1-Vinylpyrene (100 mg, 0.4 mmol) was added into a dichloromethane (CH_2Cl_2) (10 mL) solution containing G−1 (36 mg, 0.04 mmol) at room temperature, and the color of that solution changed from purple to yellow immediately. After stirring for 80 min, the solution was concentrated by vacuum, washed three times with acetone, and dried under vacuum to obtain YGTZ−1, a khaki solid. ^{1}H NMR (600 MHz, Chloroform-*d*): δ 8.39 (d, J = 9.2 Hz, 1H), 8.24−8.14 (m, 4H), 8.11 (d, J = 9.2 Hz, 1H), 8.05 (s, 2H), 8.00 (t, J = 7.6 Hz, 1H), 7.80 (dd, J = 17.3, 11.0 Hz, 1H), 6.00 (d, J = 17.3 Hz, 1H), 5.62 (d, J = 11.0 Hz, 1H), 2.33−1.79 (m, 3H), 1.76−0.63 (m, 6H). ^{13}C NMR (151 MHz, Chloroform-*d*): δ 131.47, 131.47, 130.88, 128.40, 125.03, 35.54, 35.13, 32.34, 29.80, 29.65, 27.83, 26.98, 26.90, 26.52, 26.34, 26.15.^{31}P NMR (243 MHz, Chloroform-*d*): δ 50.47, 35.49, 24.24. Anal. Calcd for $C_{53}H_{76}Cl_2P_2Ru$/C, 67.21; H, 8.09. ESI: 911.66931, 913.67566, 947.63428.

2.1.2.2. Preparation of YGTZ−2. Ph_3PCH_3I (22.5 g, 56 mmol) was dissolved in dried 200 mL THF and then KO^tBu (16.61 g, 148 mmol) was added into the solution at 0 °C. After stirring for 30 min, 1-naphthaldehyde ($C_{11}H_8O$) (5.75 g, 37 mmol) was added to the solution, stirred for 6 h, and then 100

https://doi.org/10.1021/acsomega.3c00586
ACS Omega 2023, 8, 15350−15359

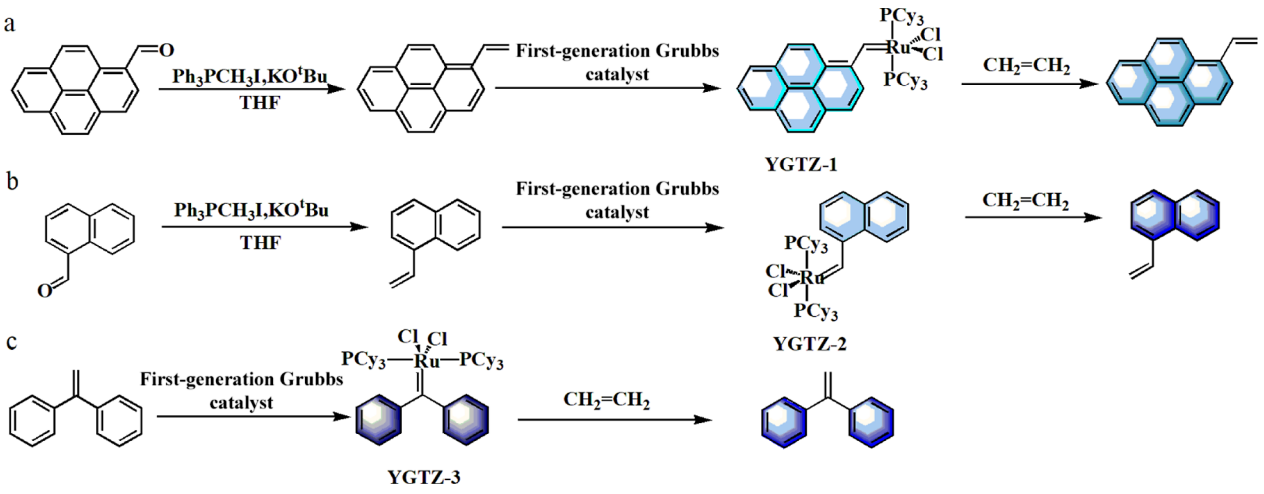

Figure 1. Design and detection mechanism of YGTZs. (a) YGTZ−1, (b) YGTZ−2, and (c) YGTZ−3.

mL of deionized water was added to quench the reaction. The product of the reaction was extracted with ethyl acetate, and the organic layer was dried with sodium sulfate anhydrous, and colorless oily liquid 1-vinylnaphthalene ($C_{12}H_{10}$) was obtained by column chromatography (developing agent: *n*-hexane/ethyl acetate = 20/1). ^{1}H NMR (600 MHz, Chloroform-*d*): δ 7.89 (d, J = 8.0 Hz, 1H), 7.61 (d, J = 8.5 Hz, 1H), 7.54 (d, J = 8.1 Hz, 1H), 7.41 (d, J = 7.1 Hz, 1H), 7.32−7.15 (m, 4H), 5.57 (s, 1H), 5.24 (s, 1H). ^{13}C NMR (151 MHz, Chloroform-*d*): δ 141.28, 135.64, 134.41, 133.62, 131.14, 128.80, 128.55, 128.14, 127.21, 126.10, 125.79, 123.80, 123.66, 117.16.

$C_{12}H_{10}$ (200 mg, 1.32 mmol) was added into CH_2Cl_2 (30 mL) solution containing G−1 (108 mg, 0.132 mmol) at room temperature, and the purple solution turned brown immediately. After stirring for 80 min, the solution was concentrated by vacuum, washed with acetone three times, and dried in vacuum to obtain YGTZ−2, a gray purple solid. ^{1}H NMR (600 MHz, Chloroform-*d*): δ 8.13 (d, J = 8.1 Hz, 1H), 7.86 (d, J = 8.7 Hz, 1H), 7.80 (d, J = 8.2 Hz, 1H), 7.63 (s, 1H), 7.61 (s, 1H), 7.52−7.51 (m, 1H), 7.49 (s, 1H), 7.46 (s, 1H), 2.39−2.17 (m, 5H), 2.08−1.68 (m, 27H), 1.51−0.83 (m, 29H). ^{13}C NMR (151 MHz, Chloroform-*d*): δ 141.28, 135.64, 134.41, 133.62, 131.14, 128.80, 128.55, 128.14, 127.21, 126.10, 125.79, 123.80, 123.66, 117.16.^{13}C NMR (151 MHz, Chloroform-*d*): δ 142.14, 141.56, 128.77, 128.52, 128.21, 126.06, 125.76, 123.76, 122.65, 35.54, 35.14, 29.78, 29.66, 27.84, 26.91, 26.53, 26.35, 26.16.^{31}P NMR (243 MHz, Chloroform-*d*): δ 51.16, 24.33. Anal. Calcd for $C_{43}H_{74}Cl_2P_2Ru$/C, 64.66; H, 8.54. ESI: 841.44177, 873.44751, 876.45105.

2.1.2.3. Preparation of YGTZ−3. 1,1-Diphenylethene ($C_{14}H_{12}$) (237 mg, 1.32 mmol) was added into CH_2Cl_2 (30 mL) solution containing G−1 (108 mg, 0.132 mmol) at room temperature, and the purple solution immediately turned black-purple. After stirring for 80 min, the solution was concentrated by vacuum, washed three times with acetone, and dried in vacuum to obtain YGTZ−3, a brown liquid. ^{1}H NMR (600 MHz, Chloroform-*d*): δ 7.37−7.35 (m, 5H), 7.35 (s, 3H), 7.34 (d, J = 2.6 Hz, 2H), 5.48 (s, 2H), 2.43−1.43 (m, 2H), 1.27 (s, 1H). ^{13}C NMR (151 MHz, Chloroform-*d*): δ 150.26, 141.66, 128.35, 114.44, 53.67, 51.71, 50.84, 35.43 (d, *J* = 60.8 Hz), 30.99, 27.14, 26.42 (d, *J* = 26.2 Hz). ^{31}P NMR (243 MHz, Chloroform-*d*): δ 50.48, 35.70, 24.25. Anal. Calcd for $C_{49}H_{76}Cl_2P_2Ru$/C, 65.46; H, 8.52. ESI: 873.46246, 893.52704, 895.69330.

2.2. Test and Characterization. *2.2.1. Chemical Structure Characterization.* Fourier transform infrared (FT-IR) spectroscopy (Nicolet IS 50, Thermo Fisher Scientific, USA) was used to characterize the structure of the compounds. The spectrum range was from 700 to 3200 cm^{-1} at a resolution of 4 cm^{-1}.

^{1}H, ^{13}C, and ^{31}P nuclear magnetic resonance (NMR) spectroscopies (Ascend 600 MHz, Bruker, Germany) were also used to characterize the structure of the compounds. It mainly determines the structure of the compound by measuring the number and distribution of hydrogen atoms at each peak position. Deuterated chloroform ($CDCl_3$) was used as the solvent. ^{13}C NMR spectroscopy is an analytical technique that analyzes nuclear magnetic resonance signals containing carbon by measuring them and making judgments about the structure based on their intensity. ^{31}P NMR spectroscopy allows accurate detection of changes in phosphorus-containing compounds in chemical reactions and enables monitoring of synthetic reaction processes. Molecular weight and structure of compounds were also determined using a Thermo Scientific Q Exactive combined with a quadrupole Orbitrap mass spectrometer.

2.2.2. Response of Different Concentrations of YGTZ−1 on Ethylene Gas. The solutions of YGTZ−1 of 250, 200, 150, 100, 50, 25, 12.5, 6.25, 3.13, and 1.57 μmol/L concentrations were prepared by CH_2Cl_2 as the solvent. 2 mL solution of YGTZ−1 was put into 7 mL glass bottles separately, then, 1 mL ethylene gas was injected slowly. Fluorescence intensity of the solution of YGTZ−1 was measured by a fluorescence spectrophotometer (excitation wavelength was 365 nm and wavelength range was 380−600 nm). The purpose of the experiment was to study the fluorescence response of YGTZ-1 to the presence of ethylene gas and to determine the sensitivity of the compound to changes in gas concentration.

2.2.3. Response of YGTZ−1 to Ethylene with Different Volumes. The solution of YGTZ−1, that is 12.5 μmol/L, was prepared using CH_2Cl_2 as the solvent. 2 mL of the YGTZ-1 solution was added to a 7 mL glass bottle and then ethylene gas was injected slowly for 2, 4, 6, 8, 10, 12, 14, 16, 18, 20, 22, 24, 26, 28, and 30 s. The fluorescence intensity of the YGTZ-1 solution was measured using a fluorescence spectrophotometer with an excitation wavelength of 365 nm and a wavelength range of 380−600 nm.

https://doi.org/10.1021/acsomega.3c00586
ACS Omega 2023, 8, 15350−15359

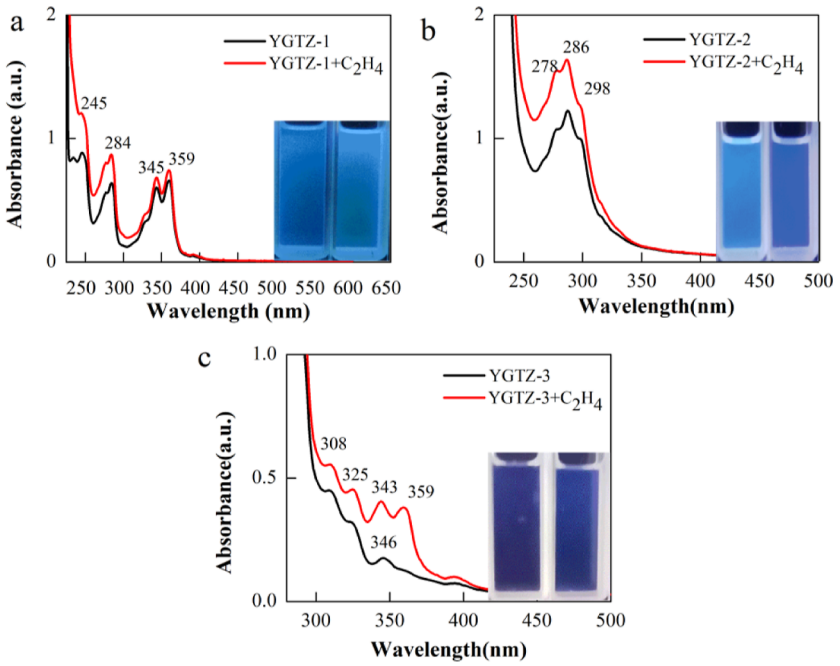

Figure 2. UV absorption spectra of YGTZs before and after adding ethylene. (a)YGTZ−1, (b) YGTZ−2, and (c) YGTZ−3. Inset: comparison photograph of solution before and after injecting 2 mL ethylene under a portable UV lamp irradiation.

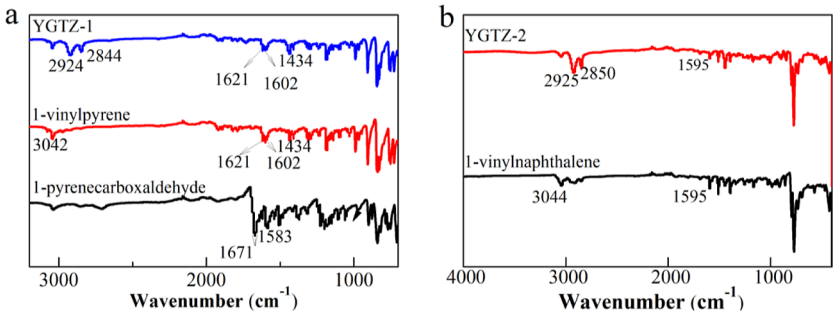

Figure 3. Infrared absorption spectra of YGTZs in the 700−3200 cm^{-1} region. (a) YGTZ−1 and (b) YGTZ−2.

2.2.4. Time Response of YGTZ−1 to Ethylene Gas. After preparing 12.5 μmol/L solution of YGTZ−1, ethylene gas was slowly injected into the solution at intervals of 1, 2, 3, 4, 5, 6, 7, 8, 9, 10, 15, 20, 25, and 30 min to measure the fluorescence intensity of the solution of YGTZ−1 by a fluorescence spectrophotometer (excitation wavelength was 365 nm and wavelength range was 380−600 nm).

The YGTZ-2 and YGTZ-3 are also the same test method, except for the way to calculate the amount of ethylene gas, the probe concentration and time dependence of the test method are the same.

2.3. Detection of Ethylene Release during Fruit Ripening. This experiment is designed to measure the amount of ethylene gas released by cherry tomatoes over a period of time. The experiment involves incubating the tomatoes in a closed container and then taking gas samples from the headspace at different time points (2, 4, 6, 8, and 10 h). The gas samples are then bubbled into a solution of 200 μmol/L YGTZ-2 in a colorimetric dish and shaken for 3 min to dissolve any ethylene gas present. The fluorescence intensity of the solution is then measured using a fluorescence spectrophotometer with an excitation wavelength of 365 nm and a wavelength range of 380−600 nm. By comparing the fluorescence intensity of the solution to a calibration curve generated using known concentrations of ethylene gas, the amount of ethylene released by the tomatoes can be determined.

3. RESULTS AND DISCUSSION

3.1. Design and Synthesis of YGTZs. Three different G−1 type fluorescent probes were designed and prepared for detecting ethylene. The probes were labeled with 1-vinylpyrene (YGTZ-1), 1-vinylnaphthalene (YGTZ-2), and 1,1-diphenylethene (YGTZ-3). The probes contain a metal complex of ruthenium that suppresses the fluorescence of the

Table 1. Characteristic Absorption Peaks and Functional Group Position

group	vibration types	absorption frequency	intensity
−CHO	stretching vibration	2852, 2709	weak, width
=CH	stretching vibration	3042	weak, tip
−CH	stretching vibration	2924, 2844	strength, tip
=CH	bending vibration	1621, 1602, 1595	weak, tip
−CHO	stretching vibration	1671	strength, tip

https://doi.org/10.1021/acsomega.3c00586
ACS Omega 2023, 8, 15350−15359

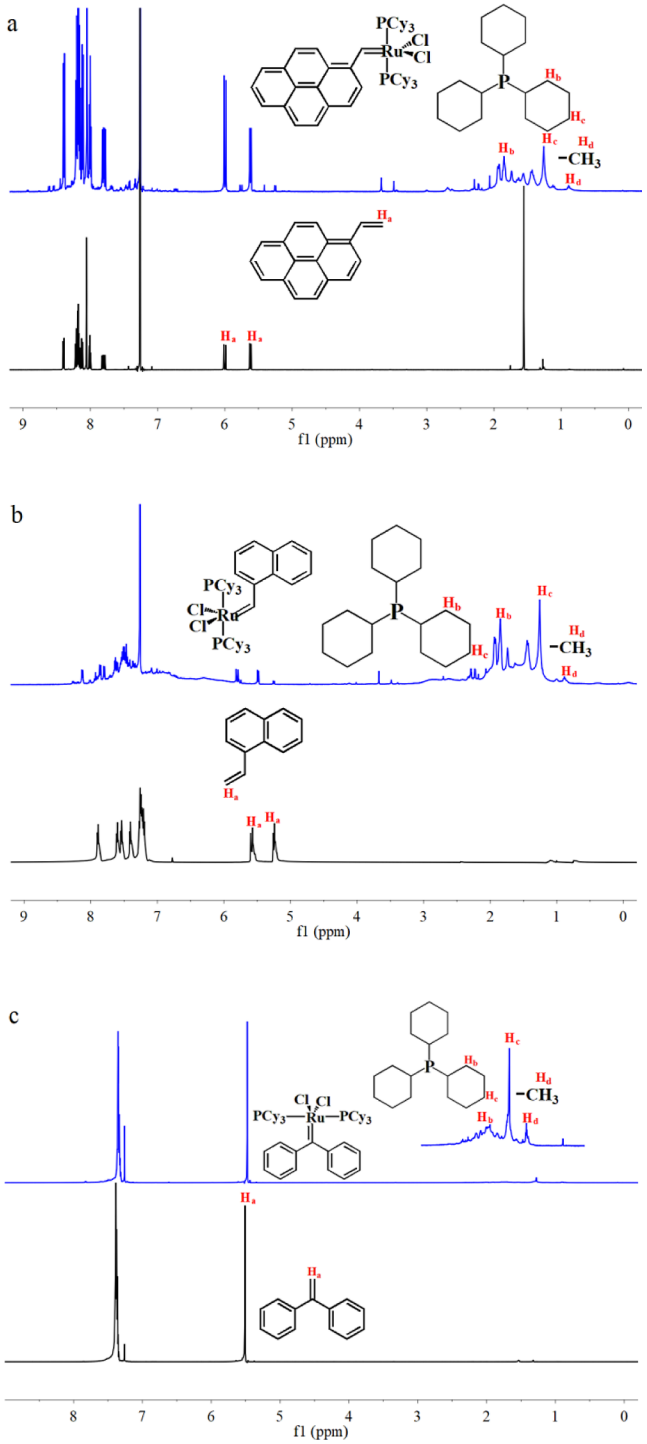

Figure 4. 1H NMR spectra of YGTZs. (a) YGTZ−1, (b) YGTZ−2, and (c) YGTZ−3.

probes through an intramolecular charge transfer effect.[31] When the probes encounter ethylene gas, the fluorophores are released, and the fluorescence of the probes is enhanced, resulting in a color change visible to the naked eye. The detection effect of YGTZ-1 to ethylene was reported in the literature and the other two probes were designed based on similar structures and fluorescence quantum effects with YGTZ-1. YGTZ-2 and YGTZ-3 showed a color change from light blue to dark blue and from dark purple to dark blue, respectively, when they encountered ethylene gas under irradiation of a 365 nm UV lamp (Figure 1). The use of 1,1-diphenylethene in YGTZ-3 was expected to inhibit the reaction of the probe with active molecules in the air to some extent.[32]

The UV absorption spectra of YGTZs before and after reacting with ethylene are shown in Figure 2. The illustration is the comparison image before and after the solution is injected into the ethylene gas. The fluorescent probes showed weak absorbance relatively which suggested the effective absorbance quench by energy transfer between the fluorophore and Ru center.[31] After YGTZ−1 reacted with ethylene, the color of the solution of YGTZ−1 changed from dark blue to bright blue. Meanwhile, the absorption intensity at 245, 284, 345, and 359 nm increased, and the intensity at 245 nm increased most obviously, as shown in Figure 2a. This phenomenon indicated that YGTZ−1 reacted with ethylene to release 1-vinylpyrene, and the fluorescence of the solution was enhanced. Identically, Figure 2b shows that the absorption intensity at 278, 286, and 298 nm increased after the reaction of YGTZ−2 with ethylene gas, and the color of the solution of YGTZ−2 changed from light blue to dark blue. This phenomenon also indicated that YGTZ−2 reacted with ethylene gas to release 1-vinylnaphthalene, and fluorescence of the solution was enhanced. In Figure 2c, the color of the YGTZ−3 solution changed from purple to dark blue. The absorption intensity of YGTZ−3 at 308, 325, and 343 nm increased. Meanwhile, a new absorption peak appeared at 359 nm, which moved to the long wave direction and exhibited a red shift. This phenomenon is due to the departure of the Ru group after YGTZ-3 encounters ethylene gas, releasing the fluorophore 1,1-diphenylethene. The principle of fluorescence quenching was the same as the above two fluorescent probes. After reacting with ethylene, the fluorophore 1,1-diphenylethene was released, and the fluorescence of the solution was enhanced.

In summary, the UV absorption spectra of YGTZs before and after reacting with ethylene show a clear difference, indicating the release of the respective fluorophore and the enhancement of fluorescence intensity after the reaction with ethylene. The color change of the solutions of the three YGTZ fluorescent probes also confirms the successful reaction with ethylene. The principle of fluorescence quenching is based on the intramolecular charge transfer effect between the fluorophore and the ruthenium complex in YGTZs.[33]

3.1.1. FT-IR Profile of the YGTZs. Figure 3 shows the infrared absorption spectra of YGTZs in the 700−3200 cm^{-1} region. In Figure 3a, it can be observed that the stretching vibration peaks of −CHO in 1-pyrenecarboxaldehyde disappeared at 1671 and 1583 cm^{-1} after the Wittig reaction. Additionally, the stretching vibration absorption peak of ═CH at 3046 cm^{-1} and bending vibration absorption peaks of ═CH at 1621 and 1602 cm^{-1} appeared, indicating the successful submethylation of −CHO. The disappeared stretching vibration absorption peak of ═CH at 3046 cm^{-1} indicates that G−1 reacted successfully with the intermediate product 1-vinylpyrene. The absorbances of the bands at 2924 and 2844 cm^{-1} are related to the stretching vibration of −CH, which confirms the successful synthesis of YGTZ-1. Similarly, Figure 3b shows the infrared absorption spectra of YGTZ−2 in the 700−3200 cm^{-1} region. After 1-vinylnaphthalene and G−1 reacted, the stretching vibration absorption peak of ═CH at 3044 cm^{-1} disappeared, and the −CH stretching vibration absorption peaks of 2925 and 2850 cm^{-1} appeared. These peaks confirm the successful synthesis of YGTZ−2. The

https://doi.org/10.1021/acsomega.3c00586
ACS Omega 2023, 8, 15350−15359

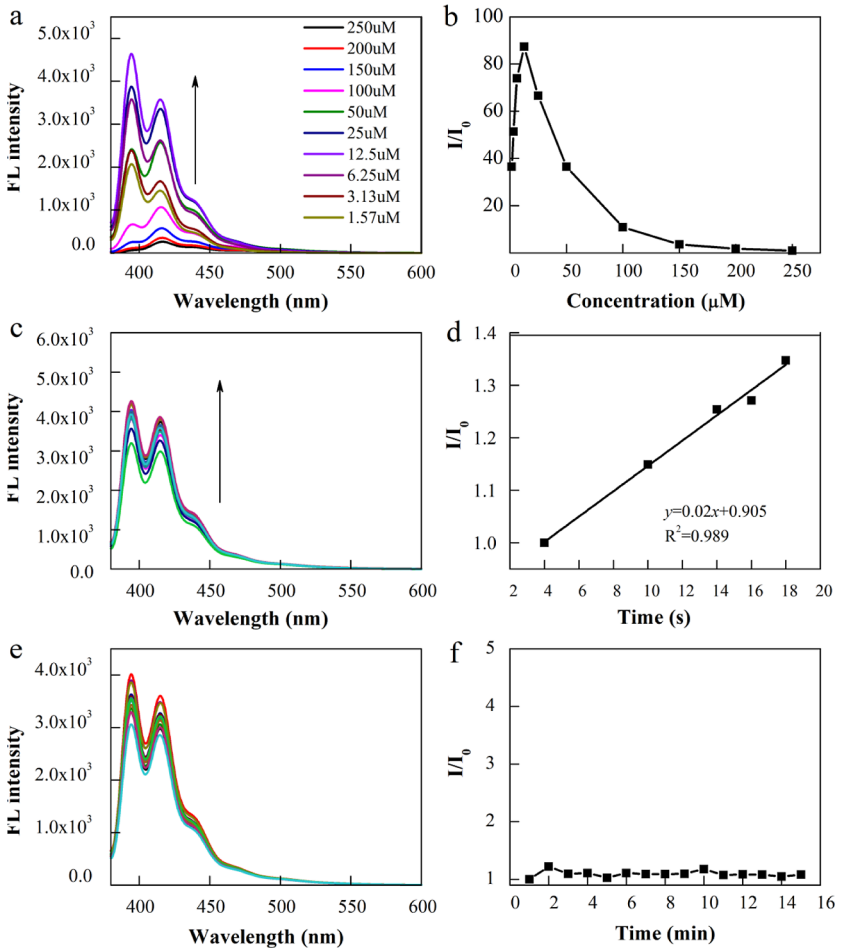

Figure 5. Fluorescence response of YGTZ−1. (a) Emission spectra of YGTZ−1 with different concentrations (1.57−250 μM) after injecting into 1.0 mL ethylene gas; (b) curve of I/I_0 versus YGTZ−1 concentration, where I_0 represents the initial fluorescence intensity measured in each group at 395 nm (λex = 365 nm), and I represents the fluorescence intensity at that concentration; (c) fluorescence spectra/intensity of 12.5 μM YGTZ−1 solution with injecting ethylene at different periods (4−18 s); (d) linear relationship between I/I_0 and ethylene in different periods; (e) emission spectra of 12.5 μM YGTZ−1 solution after injecting 20 s ethylene in 15 min; and (f) relationship between I/I_0 and reaction times.

characteristic absorption peak and functional group position of FT-IR are also listed in Table 1.

3.1.2. NMR Spectra of YGTZs. ^{1}H NMR spectra provide further evidence for the successful synthesis of YGTZs. In Figure 4a, the appearance of new peaks (H_b = 2.33−1.79 ppm, H_c = 1.76−1.41 ppm, H_d = 1.20−0.85 ppm) indicated the successful composition of YGTZ-1. Similarly, in Figure 4b, the appearance of new peaks (H_b = 2.39−2.17 ppm, H_c = 2.08−1.68 ppm, H_d = 1.5−0.83 ppm) indicated the successful composition of YGTZ−2. Finally, in Figure 4c, the appearance of new peaks (H_b, H_c = 2.43−1.43 ppm, H_d = 1.27 ppm) indicated the successful composition of YGTZ−3. The chemical shifts at 6.00, 5.62, 5.57, and 5.51 ppm were assigned to the =CH in each of the YGTZs. The presence of $-CH_3$ groups was also confirmed by the chemical shifts at 35.54, 32.34, 27.83, and 26.98 ppm in YGTZ−1(Figure. s2) and at 35.54, 29.78, 27.84, and 26.53 ppm in YGTZ−2 and YGTZ−3 (Figures S6, S9). The chemical shift at 35.49 ppm in YGTZ−1 and at 35.70 ppm in YGTZ−3 indicated the existence of P-atoms (Figures S3, S10). Overall, ^{1}H NMR, ^{13}C NMR, ^{31}P NMR spectra provide complementary evidence to FT-IR spectra for the successful synthesis of YGTZs.

3.2. Fluorescence Response of YGTZs. *3.2.1. Fluorescence Response of YGTZ−1.* Figure 5 presents the performance test results of the reaction between YGTZ-1 and ethylene gas. In Figure 5a, the fluorescence intensity of emission spectra of YGTZ-1 at different concentrations (ranging from 1.57 to 250 μM) injected into 1.0 mL of ethylene gas is shown. The fluorescence intensity changes with different concentrations of YGTZ-1. Figure 5b shows the relationship between the concentration of YGTZ-1 and the ratio of fluorescence intensity to the initial fluorescence intensity (I/I_0). The fluorescence intensity of YGTZ-1 increases with increasing the concentration up to 12.5 μM, beyond which the fluorescence intensity decreases due to aggregation-induced self-quenching.[34] Figure 5c depicts the fluorescence intensity of YGTZ-1 (12.5 μM) solution injected with ethylene gas for different time intervals (ranging from 4 to 18 s). The fluorescence intensity of the solution increases at 395 nm as the injected ethylene gas increases. Figure 5d shows the linear relationship between fluorescence intensity and ethylene content, with a correlation coefficient of R^2 = 0.989. As the amount of ethylene gas increases, the fluorophore 1-vinylpyrene is gradually released, leading to an increase in the fluorescence intensity of the YGTZ-1 solution. Figure 5e displays the emission spectra of the YGTZ-1 solution at different times, showing that the fluorescence intensity gradually increases in the first 3 min and then remains steady for the next 10 min, indicating that

https://doi.org/10.1021/acsomega.3c00586
ACS Omega 2023, 8, 15350−15359

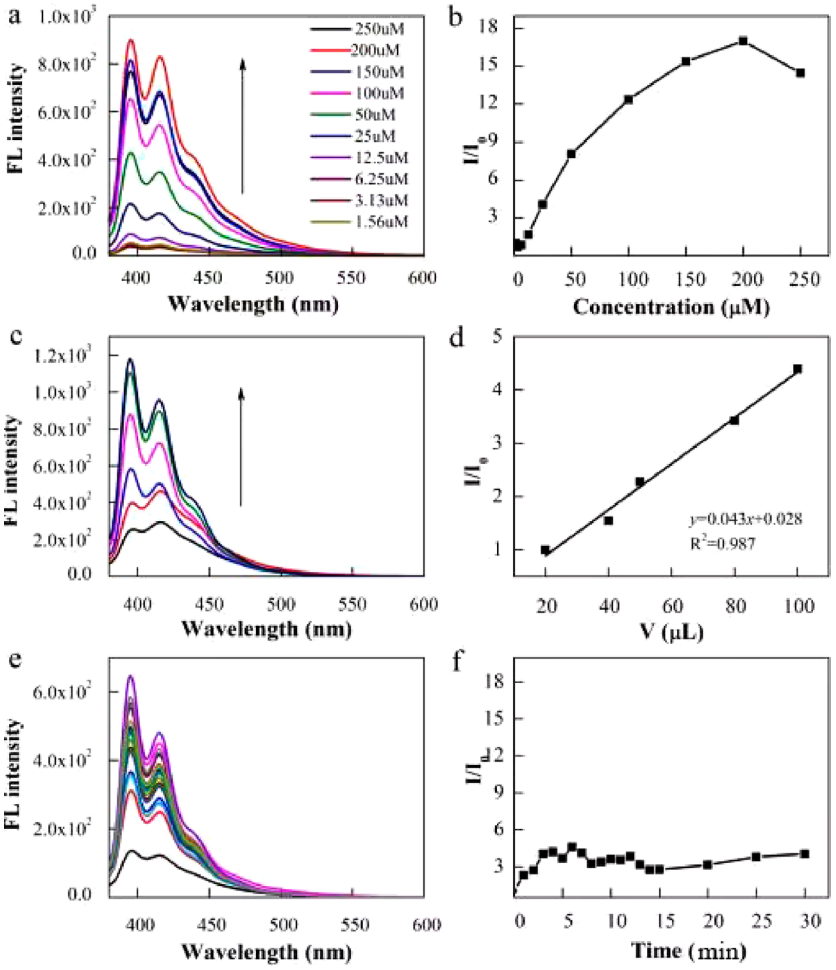

Figure 6. Fluorescence response of YGTZ−2. (a) Emission spectra of YGTZ−2 with different concentrations (1.57−250 μM) after injecting into 0.6 mL ethylene gas; (b) curve of I/I_0 versus YGTZ−2 concentration, where I_0 represents the initial fluorescence intensity measured in each group at 395 nm (λex = 365 nm), and I represents the fluorescence intensity at that concentration; (c) fluorescence spectra/intensity of 50 μM YGTZ−2 solution with injecting different volumes of ethylene; (d) linear relationship between I/I_0 and ethylene in different volumes of ethylene; (e) emission spectra of 50 μM YGTZ−2 solution after injecting 10 mL ethylene gas in 30 min; and (f) relationship between I/I_0 and reaction times.

YGTZ-1 has good stability. Finally, Figure 5f demonstrates that the fluorescence performance of YGTZ-1 is stable and less affected by visible light.

3.2.2. Fluorescence Response of YGTZ−2. Figure 6 shows the response of YGTZ−2 to ethylene gas. The fluorescence intensity of emission spectra in YGTZ−2 with different concentrations (1.57−250 μM) after being injected into 0.6 mL ethylene gas is shown in Figure 6a. The result shows that fluorescence intensity of YGTZ−2 increases gradually with the concentration increasing. The fluorescence intensity goes up to the highest when the YGTZ−2 concentration reaches 200 μM, as shown in Figure 6b. Since the molecular weight of 1-vinylnaphthalene is smaller than that of 1-vinylpyrene, it did not undergo significant aggregation-induced self-quenching. The intensity of the solution of YGTZ-2 decreased only when the concentration of the solution of YGTZ-2 exceeded 200 μM. Figure 6c shows the fluorescence spectrum of YGTZ−2 with 200 μM concentration injected into different volumes of ethylene (20−100 μL), respectively. The relationship between volume of ethylene and I/I_0 is shown in Figure 6d. The fluorescence intensity of the YGTZ−2 solution at 395 nm increases with the volume of ethylene increasing, and there is a well linear relationship and the correlation coefficient is R^2 = 0.987. As the amount of ethylene gas released increases, the fluorophore 1-vinylnaphthalene is released gradually and the solution of YGTZ-2 fluorescence is enhanced. Figure 6e and Figure 6f shows the fluorescence emission spectra and the fluorescence intensity of YGTZ−2 solution after being bubbled into 10 mL ethylene at different times. As shown on Figure 6f, the fluorescence intensity of the YGTZ−2 solution is the highest when time reaches 3 min and then stabilizes gradually for about 8 min. The fluctuation of I/I_0 in different times could be caused by solvent evaporation. It is also possible that YGTZ-2 is influenced greatly by visible light and the fluorescence properties of the solution of YGTZ-2 are less stable.

In summary, Figure 6 demonstrates the response of YGTZ-2 to ethylene gas through fluorescence intensity measurements. The results show that as the concentration of YGTZ-2 increases, the fluorescence intensity also increases until a concentration of 200 μM is reached. Additionally, the fluorescence intensity of the YGTZ-2 solution at 395 nm increases linearly with the volume of ethylene gas, indicating a proportional relationship between the two. Furthermore, the fluorescence intensity of the YGTZ-2 solution bubbled into ethylene gas reaches its maximum value after 3 min and then stabilizes for about 8 min. However, the fluctuations in fluorescence intensity may be due to solvent evaporation and

https://doi.org/10.1021/acsomega.3c00586
ACS Omega 2023, 8, 15350−15359

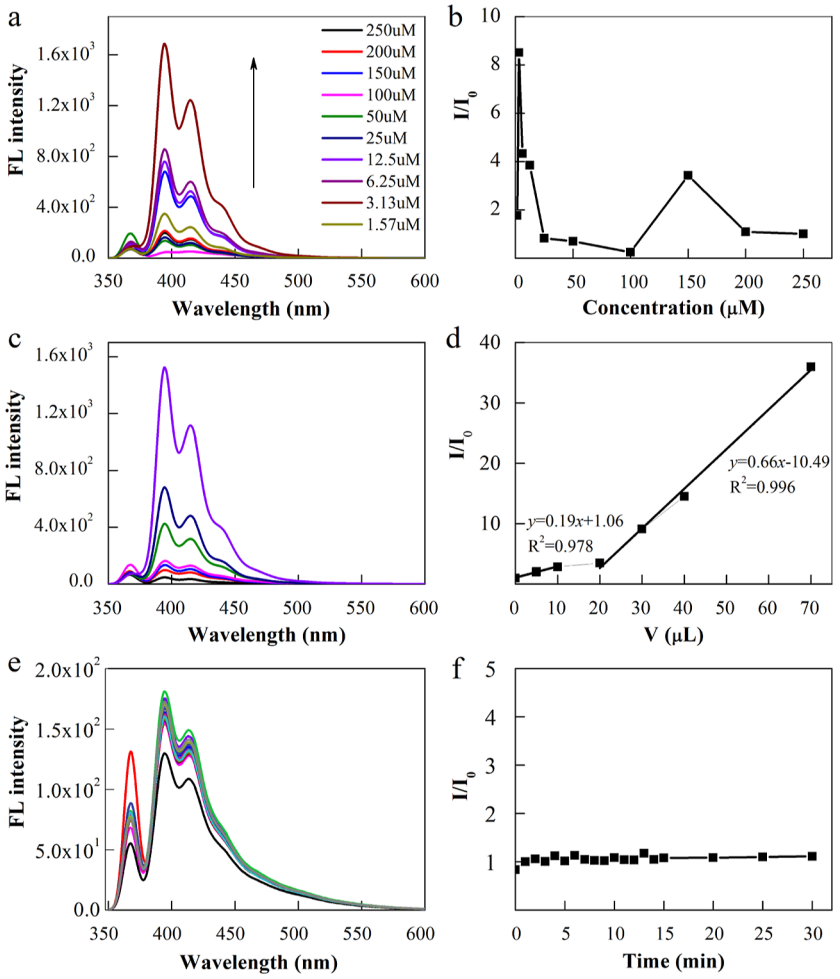

Figure 7. Fluorescence response of YGTZ−3. (a) Emission spectra of YGTZ−3 with different concentrations (1.57−250 μM) after injecting into 1.0 mL ethylene gas; (b) curve of I/I_0 versus YGTZ−3 concentration, where I_0 represents the initial fluorescence intensity measured in each group at 395 nm (λex = 365 nm), and I represents the fluorescence intensity at that concentration; (c) fluorescence intensity of 150 μM YGTZ−3 solution with injecting different volumes of ethylene; (d) linear relationship between I/I_0 and volume of ethylene (0−70 μL); (e) emission spectra of 250 μM YGTZ−3 solution after injecting 3 mL ethylene in 30 min; and (f) linear relationship between $I/I0$ and reaction times.

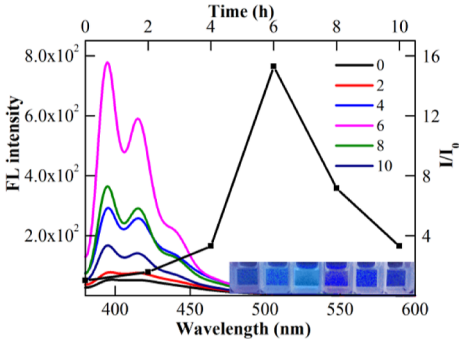

Figure 8. YGTZ−2 monitoring ethylene gas released during fruit ripening (insets represent photographs of the solution of YGTZ-2 at different times with a 365 nm UV lamp).

the influence of visible light on the fluorescence properties of YGTZ-2.

3.2.3. Fluorescence Response of YGTZ−3. Figure 7 demonstrates the performance of YGTZ-3 in response to ethylene gas. The fluorescence intensity of YGTZ-3 with different concentrations (ranging from 1.57 to 250 μM) after being injected into 1.0 mL ethylene gas is shown in Figure 7a, and the relationship between the YGTZ-3 concentration and I/I_0 is presented in Figure 7b. The overall fluorescence intensity of YGTZ-3 decreases with increasing the concentration in the range of 3.13−100 μM, with two optimal concentrations of 150 and 3.13 μM being observed. The authors suggest that the presence of incomplete 1,1-diphenylethene in YGTZ-3 may have affected the experimental results. For subsequent experiments, the authors select 150 μM of YGTZ-3. Figure 7c shows the fluorescence intensity of YGTZ-3 (150 μM) injected into different volumes of ethylene gas (ranging from 0 to 70 μL), and Figure 7d displays the relationship between the volume of ethylene gas and I/I_0. The fluorescence intensity increases with the volume of ethylene gas and exhibits a linear relationship between 20 and 70 μL, with a high correlation coefficient (R^2 = 0.993). This indicates that as the amount of ethylene gas released increases, the fluorescence of the YGTZ-3 solution enhances. Furthermore, Figure 7e depicts the fluorescence intensity of the YGTZ-3 solution after being bubbled into 3 mL of ethylene gas at different times, and Figure 7f shows the relationship between I/I_0 and reaction times. The fluorescence intensity reaches its peak at 2 min and then stabilizes, indicating that YGTZ-3 is

https://doi.org/10.1021/acsomega.3c00586
ACS Omega 2023, 8, 15350−15359

less affected by visible light, and its fluorescence performance is stable.

3.3. Monitoring the Mature Process of Cherry Tomatoes Using YGTZ−2. Figure 8 shows the results of monitoring ethylene release of cherry tomatoes during storage using YGTZ-2. The fluorescence intensity of YGTZ-2 solution gradually increased with the storage time, indicating an increase in ethylene release. The ethylene release rate increased in the first 6 h and then decreased in the last 4 h. This trend suggests that ethylene release is related to the respiration rate of the cherry tomatoes. The increase in ethylene release over time can accelerate the ripening and spoilage of the fruit. The decrease in ethylene release in the later hours may be related to the respiratory process of the cherry tomatoes themselves, which requires further investigation. Overall, YGTZ-2 was effective in monitoring the ethylene release of cherry tomatoes during storage, which can help in optimizing the storage conditions to prolong the shelf life of the fruit.

4. CONCLUSIONS

The development of these fluorescence probes offers an effective tool for the detection and monitoring of ethylene gas. This is particularly important in the agricultural and horticultural industries, where ethylene gas can have a significant impact on the quality and shelf life of produce. The use of these probes can help in identifying ethylene gas levels and prevent spoilage, resulting in less waste and increased efficiency. Furthermore, the detection limit of these probes is relatively low, indicating their potential for use in sensitive and precise applications. Overall, this research opens up new possibilities for the development of efficient, cost-effective, and non-destructive methods for the detection and monitoring of ethylene gas.

■ ASSOCIATED CONTENT

Supporting Information

The Supporting Information is available free of charge at https://pubs.acs.org/doi/10.1021/acsomega.3c00586.

^{13}C NMR, ^{31}P NMR, and MS spectra (PDF)

■ AUTHOR INFORMATION

Corresponding Author

Peng Tu − *College of Science, Gansu Agricultural University, Lanzhou 730070, PR China*; Email: tupeng815@163.com

Authors

Yanyan Yang − *College of Science, Gansu Agricultural University, Lanzhou 730070, PR China*; orcid.org/0009-0002-8457-728X

Hongxia Bian − *College of Science, Gansu Agricultural University, Lanzhou 730070, PR China*

Zhilong Jia − *College of Science, Gansu Agricultural University, Lanzhou 730070, PR China*

Complete contact information is available at: https://pubs.acs.org/10.1021/acsomega.3c00586

Funding

Financial Support from The Science and Technology Innovation Foundation of Gansu Agricultural University - Young Mentor Support Fund (GAU-QDFC-2020-06) and Natural Science Foundation of Gansu Province (22JR5RA866).

Notes

The authors declare no competing financial interest.

The data presented in this study are available on request from the corresponding author.

■ ACKNOWLEDGMENTS

P.Tu and H. Bian designed and supervised the experiments. Y. Yang conducted the experiments. Z. Jia advised on the optimization of the reaction. H. Bian helped in providing the various tests. Y. Yang wrote the manuscript. H. Bian revised the manuscript. P. Tu and H. Bian provided the funds.

■ REFERENCES

(1) Bo-Wen, C.; Liu, J.; Peng, Z.; Xiao-Rui, G. *Effects of Exogenous Ethylene on Physiology and Alkaloid Accumulations in Catharanthus Roseus*; Bulletin of Botanical Research, 2018.

(2) Wang, L. C.; Li, H.; Ecker, J. R. Ethylene Biosynthesis and Signaling Networks. *The Plant Cell* **2002**, *14*, S131−S151.

(3) Pattyn, J.; Vaughan-Hirsch, J.; Van de Poel, B. The Regulation of Ethylene Biosynthesis: A Complex Multilevel Control Circuitry. *New Phytol.* **2021**, *229*, 770−782.

(4) Jiang, Y.; Fu, J. Ethylene Regulation of Fruit Ripening: Molecular Aspects. *Plant Growth Regul.* **2000**, *30*, 193−200.

(5) Hu, B.; Sun, D.-W.; Pu, H.; Wei, Q. Recent Advances in Detecting and Regulating Ethylene Concentrations for Shelf-Life Extension and Maturity Control of Fruit: A Review. *Trends Food Sci. Technol.* **2019**, *91*, 66−82.

(6) Zhang, S.; Wang, X.; Xu, Z.; Shi, P.; Gu, M.; Kang, T.; Li, Q.; Zhang, D.; Zhao, C. PrupeFUL4 Regulates Ripening and Softening of Peach Fruits through Ethylene Biosynthesis. *Acta Physiol Plant* **2022**, *44*, 23.

(7) Liu, Y.; Tang, M.; Liu, M.; Su, D.; Chen, J.; Gao, Y.; Bouzayen, M.; Li, Z. The Molecular Regulation of Ethylene in Fruit Ripening. *Small Methods* **2020**, *4*, 1900485.

(8) Xiong, A. DOUBLE-ANTISENSE ACC OXIDASE AND ACC SYNTHASE FUSION GENE INTRODUCED INTO TOMATO BY AGROBACTERIUM-MEDIATED TRANSFORMATION AND ANALYSIS THE ETHYLENE PRODUCTION OF TRANSGENIC PLANTS. *acta biologiae experimentalis sinica* **2003**, *36*, 428−434.

(9) Caprioli, F.; Quercia, L. Ethylene Detection Methods in Post-Harvest Technology: A Review. *Sens. Actuators, B* **2014**, *203*, 187−196.

(10) Cristescu, S. M.; Mandon, J.; Arslanov, D.; De Pessemier, J.; Hermans, C.; Harren, F. J. M. Current Methods for Detecting Ethylene in Plants. *Annals of Botany* **2013**, *111*, 347−360.

(11) Chen, X.; Wreyford, R.; Nasiri, N. Recent Advances in Ethylene Gas Detection. *Materials* **2022**, *15*, 5813.

(12) Noh, H.; Lim, T.; Park, B. Y.; Han, M. S. A Fluorescence-Based High-Throughput Screening Method for Olefin Metathesis Using a Ratiometric Fluorescent Probe. *Org. Lett.* **2020**, *22*, 1703−1708.

(13) Yi, S.; Li, H.; Liu, X. Enhanced Fluorescence Quenching for *p*-Nitrophenol in Imidazolium Ionic Liquids Using a Europium-Based Fluorescent Probe. *Rsc Adv* **2022**, *12*, 10915−10923.

(14) Pike, S. J.; Hunter, C. A. Fluorescent and Colorimetric Molecular Recognition Probe for Hydrogen Bond Acceptors. *Org. Biomol. Chem.* **2017**, *15*, 9603−9610.

(15) Katla, J.; Kanvah, S. Styrylisoxazole-Based Fluorescent Probes for the Detection of Hydrogen Sulfide. *Photochem. Photobiol. Sci.* **2018**, *17*, 42−50.

(16) Li, Y.; Guo, D.; Ruan, W. Photoluminescence and Fluorescent Sensing: Application of the Fundamental Principles of Photochemistry. *Univ. Chem* **2019**, *34*, 45.

(17) Ashkar, M. A.; Chandhru, M.; Sundar, M.; Kutti Rani, S.; Vasimalai, N. The Rapid Synthesis of Intrinsic Green-Fluorescent Poly(Pyrogallol)-Derived Carbon Dots for Amoxicillin Drug Sensing in Clinical Samples. *New J. Chem.* **2022**, *46*, 18805−18814.

(18) Vasimalai, N.; Fernández-Argüelles, M. T.; Espiña, B. Detection of Sulfide Using Mercapto Tetrazine-Protected Fluorescent Gold

Nanodots: Preparation of Paper-Based Testing Kit for On-Site Monitoring. *ACS Appl. Mater. Interfaces* **2018**, *10*, 1634−1645.
(19) Varatharajan, P.; Banu, I. S.; Mamat, M. H.; Vasimalai, N. Hydrothermal Synthesis of Orange Fluorescent Carbon Dots and Their Application in Fabrication of Warm WLEDs and Fluorescent Ink. *Physica B: Condensed Matter* **2023**, *654*, 414703.
(20) Maruthupandi, M.; Thiruppathi, D.; Vasimalai, N. One Minute Synthesis of Green Fluorescent Copper Nanocluster: The Preparation of Smartphone Aided Paper-Based Kit for on-Site Monitoring of Nanomolar Level Mercury and Sulfide Ions in Environmental Samples. *J. Hazard. Mater.* **2020**, *392*, 122294.
(21) Maruthupandi, M.; Varatharajan, P.; Shameem Banu, I. B.; Hafiz Mamat, M.; Vasimalai, N. White Light Emitting Diode and Anti-Counterfeiting Applications of Microwave Assisted Synthesized Green Fluorescent Carbon Dots Derived from Waste Curry Leaves. *Results in Optics* **2022**, *8*, 100249.
(22) Vasimalai, N.; Fernandez-Arguelles, M. T. Novel One-Pot and Facile Room Temperature Synthesis of Gold Nanodots and Application as Highly Sensitive and Selective Probes for Cyanide Detection. *Nanotechnology* **2016**, *27*, 475505.
(23) Esser, B.; Swager, T. M. Detection of Ethylene Gas by Fluorescence Turn-On of a Conjugated Polymer. *Angew. Chem., Int. Ed.* **2010**, *49*, 8872−8875.
(24) Tabassum, S.; Kumar, D. P.; Kumar, R. Copper Complex-Coated Nanopatterned Fiber-Tip Guided Mode Resonance Device for Selective Detection of Ethylene. *IEEE Sensors J* **2021**, *21*, 17420−17429.
(25) Green, O.; Smith, N. A.; Ellis, A. B.; Burstyn, J. N. $AgBF_4$-Impregnated Poly(Vinyl Phenyl Ketone): An Ethylene Sensing Film. *J. Am. Chem. Soc.* **2004**, *126*, 5952−5953.
(26) Hitomi, Y.; Nagai, T.; Kodera, M. A Silver Complex with an N,S,S-Macrocyclic Ligand Bearing an Anthracene Pendant Arm for Optical Ethylene Monitoring. *Chem. Commun.* **2012**, *48*, 10392.
(27) Marshall, M. E.; Mohler, J. L.; Edmonds, K.; Williams, B.; Butler, K.; Ryles, M.; Weiss, L.; Urban, D.; Bueschen, A.; Markiewicz, M.; Cloud, G. An Updated Review of the Clinical Development of Coumarin (1,2-Benzopyrone) and 7-Hydroxycoumarin. *J Cancer Res Clin Oncol* **1994**, *120*, S39−S42.
(28) Chen, Y.; Yan, W.; Guo, D.; Li, Y.; Li, J.; Liu, H.; Wei, L.; Yu, N.; Wang, B.; Zheng, Y.; Jing, M.; Zhao, J.; Ye, Y. An Activity-Based Sensing Fluorogenic Probe for Monitoring Ethylene in Living Cells and Plants. *Angew Chem Int Ed* **2021**, *60*, 21934−21942.
(29) Sun, M.; Yang, X.; Zhang, Y.; Wang, S.; Wong, M. W.; Ni, R. Rapid and Visual Detection and Quantitation of Ethylene Released from Ripening Fruits: The New Use of Grubbs Catalyst. *J. Agric. Food Chem.* **2019**, *67*, 507.
(30) Majumdar, R.; Carlini, C.; Rosato, N.; Houben, J. Chiroptical and Fluorescence Properties of Copolymers of (−)Menthyl Acrylate and (−) Menthyl Methacrylate with 1-Vinylnaphthalene. *Polymer* **1980**, *21*, 941−948.
(31) Wu, M.; Yin, C.; Fu, L.; Liu, T.; Jiang, M.; Sun, Q.; Chen, L.; Niu, N. A Biocompatible Ruthenium-Based Composite Fluorescent Probe Using Bovine Serum Albumin as a Scaffold for Ethylene Gas Detection and Its Fluorescence Imaging in Plant Tissues. *Chem. Eng. J.* **2022**, *435*, 135045.
(32) Pang, X.; Cheng, G.; Lu, S. Morphology and Thermodynamic Analysis of Composite Polymer Particles Prepared by Soap-Free Emulsion Polymerization in the Presence of Poly(Methyl Methacrylate) and Polystyrene as Biseeds. *J. Appl. Polym. Sci.* **2004**, *92*, 2675−2680.
(33) Lu, Z.; Fen, X.; Liu, L.; Zhu, Y. The review of luminescence mechanism of fluorescent probes. *Fujian Journal of Analytical Chemistry* **2017**, *26*, 1009−8143.
(34) Chen, S.; Xu, J.; Li, Y.; Peng, B.; Luo, L.; Feng, H.; Chen, Z.; Wang, Z. Research Progress of Aggregation-Caused Quenching-(ACQ)to Aggregation-Induced Emission(AIE)Transformation Based on Organic Small Molecule. *J. Org. Chem.* **2022**, *42*, 1651.

https://doi.org/10.1021/acsomega.3c00586
ACS Omega 2023, 8, 15350−15359